

The Derivation of the Fundamental Superconducting Interaction and the Phase Diagram of Cuprates

E. V. L. DE MELLO

¹ *Instituto de Física, Universidade Federal Fluminense, Niterói, RJ 24210-340, Brazil*

PACS 74.20.-z – Theories and Models of Superconducting State

PACS 74.25.Dw – Superconductivity Phase Diagram

PACS 74.72.-h – Cuprate Superconductors

Abstract. - We show that an electronic phase separation (EPS) transition described by the Cahn-Hilliard theory yields regions of low free energy forming grains of low and high charge densities. These local differences in the potential energy are studied numerically and used here for the first time as the origin of an attractive interaction that gives rise to local pair formation. The resistivity transition T_c occurs due to Josephson coupling among these superconducting regions or grains. Using this approach within the Bogoliubov-deGennes calculations we derive the Gaussian shape of T_c against the entire doping level p . We find that every pairing gap develops locally at a temperature T_p , following the relation $2\Delta/k_B T_p \approx 8.0$ in close agreement recent measurements.

Introduction. – There are increasing evidences that the charge distribution in the CuO_2 planes of the high temperature superconductors (HTSC) is microscopically inhomogeneous. Several different experiments like neutron diffraction [1–3], muon spin relaxation (μSR) [4, 5], NQR and NMR [6, 7] have detected a position dependent electronic density. These experiments indicated that such disorder is stronger on the underdoped side of the phase diagram and it is possibly related with the non Fermi liquid behavior of the normal phase. However, recent STM studies on Bi2212 reveal spatial variations of the electronic gap amplitude on a nanometer length scale even on overdoped compounds [8–10]. These data on overdoped samples, which behave as normal Fermi liquids at high temperatures, indicates that a phase separation transition may occur at temperatures not much larger than T_c . A transition at such low temperatures (of the order of 100K) is likely to be an intrinsic electronic phase separation and not due to ionic mobility.

On the theoretical side there are many predictions that hole carriers may segregate into hole-rich and hole-poor regions at low doping due to strong carrier-carrier correlation effect [11–13].

Here we deal with a completely different approach, namely, a phase separation transition driven by the minimization of the free energy [14]. As the temperature goes below the pseudogap temperature [15, 16] T^* , the phase

separation (PS) process starts. Such second order phase transition is a direct explanation to the NQR measurements [6] of two different signals coming from two different types of local doping domains as the temperature goes down. The origin of this EPS transition is the proximity to the insulator AF phase, common to all cuprates, as we derived from the principle of the competing minimum free energy [14]. When the temperature decreases below $T_{PS}(p)$, the free energy of the homogeneous system with an average doping level or charge density p becomes *higher* than the disordered one, made mainly of two values of the local charge concentration at each point \vec{r}_i . According the stripe phase measurements [1, 2] and the NQR data [6], the local values of the density $p(\vec{r}_i) \equiv p(i)$ follows a bimodal distribution [17] formed of AF domains with $p(i) \approx 0$ and high hole density domains with $p(i) \approx 2p$. These domains, clusters or grains in the Cu-O planes are of nanometer size containing 10-100 sites.

The Electronic Phase Separation. – To trace the EPS and the cluster formation we use the general theory of Cahn-Hilliard (CH) [18]. It describes how a system evolves from small fluctuations around the average charge concentration p near the phase separation temperature $T_{PS}(p)$ to a complete separation into low and high density grains, passing by intermediates configurations as the temperature decreases. The order parameter of such transition

is the difference between the temperature dependent local charge or doping concentration $p(i, T)$ and the average doping level p , i.e., $u(i, T) \equiv (p(i, T) - p)/p$. The Ginzburg-Landau (GL) free energy functional in terms of $u(i, T)$ for a given compound p near the transition temperature is given by

$$f(i, T) = \frac{1}{2}\varepsilon^2|\nabla u(i, T)|^2 + V(u(i, T)) \equiv K + V_{GL}. \quad (1)$$

Where the potential $V_{GL}(p, i, T) = A^2(T)u^2/2 + B^2u^4/4 + \dots$, $A^2(T) = \alpha(T_{PS}(p) - T)$, α and B are temperature independent parameters. ε gives the size of the grain boundaries among two distinct phases [19,20]. $V_{GL}(p, i, T)$ changes with the site position "i"; $V(u = 0) = 0$ at the grain boundaries where $u = 0$, and has two minima $V_{GL}(u, t) = -A^4(T)/B$ in the lowest and highest density sites where the order parameter assumes the value $u_{min}(T) = \pm\sqrt{A(T)/B}$. These two V_{GL} minima regions work as attractors for the holes, giving rise to the clusters and to the main point here; it creates an effective two-body attractive potential.

The CH equation can be written [21] in the form of a continuity equation of the local free energy $f(i, T)$, $\partial_t u = -\nabla \cdot \mathbf{J}$, with the current $\mathbf{J} = M\nabla(\delta f/\delta u)$, where M is the mobility or the charge transport coefficient. Therefore,

$$\frac{\partial u}{\partial t} = -M\nabla^2(\varepsilon^2\nabla^2 u + A^2(T)u - B^2u^3). \quad (2)$$

We have already made a detailed study of the CH differential equation by finite difference methods [19] which yields the density profile $u(p, i, T)$ in a 105×105 array as function of the time steps, up to the stabilization of the local densities, using parameters in the CH simulation that yield stripe [22, 23] and patchwork [20, 24, 25] patterns at intermediate time regimes.

The Fundamental Interaction. – Here we introduce a new approach in order to derive the attractive potential that segregates the holes into grains of low and high density and which will be used as an effective two-body attraction to calculate the superconducting properties. The justification to this procedure is because, given the mesoscopic size of a grain and the low doping values of the HTSC, there are very few holes in each confined region.

Consequently we follow numerically the "kinetic" and potential energy (V_{GL}) map, that are the first and second term in Eq.(1). These energy maps show that the grains, either the low and high density ones, are regions of free energy minimum, as shown in Fig.(1). This figure describes a common intermediate regime of disorder, between a homogeneous system with a Gaussian distribution of densities and a bimodal distribution for a complete phase separation, as it is shown in the inset by the histogram of local densities $p(i)$.

Following the V_{GL} values, from low temperatures up to $T_{PS}(p)$ when the grains disappear completely, we can

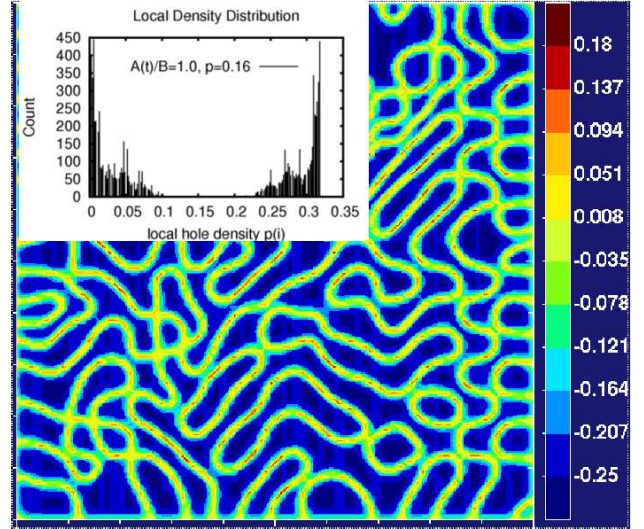


Fig. 1: (color online) The V_{GL} potential energy map showing the regions of minimum potential separated by the lines of grain boundaries. The inset is the local charge density histogram for $p = 0.16$ showing the tendency toward a bimodal charge distribution. The points marked below the inset are where we made the local density of states calculations presented in the end.

obtain the qualitative behavior of this attractive potential. Here we use parameters to reproduce the Bi2212 low temperature data of McElroy et al [8]

$$V_{GL}(p, i, T) = V(p)V(T) = (-0.9 + 2.8p)|u(i, T)|^2, \quad (3)$$

where the values are in eV, $V(p)$ is linear and vanishes at $p \approx 0.32$ following the behavior $T^*(p)$ or $T_{PS}(p)$. $V(T)$ vanishes at $T_{PS}(p)$ and increases as T decreases. The $u(i, T)$ is also parameterized in a similar way, $|u(i, T)|^2 = u(i)(1 - T/T_{PS})^{(3-T/T_{PS})}$ showing how the system becomes homogeneous at T_{PS} , and the other limit at $T = 0$ of largest phase separation with $A = B = 1$.

The energy minimum at the grains and the grain boundary energy barrier keep the holes confined forming metallic clusters with typical Fermi energies much smaller than the bulk Debye energy, the so called anti-adiabatic regime [26]. This condition with the effective hole attraction toward the cluster center is highly favorable to bipolaron formation [26]. Then the effective hole attraction, modelled by V_{GL} , is taken as the origin of the superconducting interaction in the form of a local two-body attraction in the Bogoliubov-deGennes (BdG) theory. This assumption is in agreement with the observation that a large electron mobility and a small Fermi energy produces a large Nernst Effect [27] as observed in many cuprates [28].

BdG-CH Combined Calculations. – To calculate the local superconductivity amplitude or gap function $\Delta_d(i, T)$ in a plane, we use the BdG theory with the extended Hubbard Hamiltonian in a similar fashion as we did before for a phenomenological next neighbor

potential [20, 22–25]. Except from the temperature dependent $V_{GL}(p, i, T)$, introduced here for the first time, and the granular charge density taken from the CH calculations and used as an input, all the others parameters are similar to values previously used in other calculations [14, 20, 22, 23, 25].

The *BdG-CH combined calculations* yield large superconducting amplitudes in high density grains and low or almost zero local amplitudes at regions with low densities. We define the *local superconducting temperature* $T_c(i)$ as the onset temperature for $\Delta_d(i, T)$. The largest value of $T_c(i)$ in a given compound determines the temperature $T_{on}(p)$ which marks the onset of superconductivity. Since $T_{on}(p)$ is correlated with the potential $V(p, i, T)$ it is larger in the underdoped region and decreases almost linearly as the average doping increases, similar to the Nernst effect onset temperature [22, 28] or a signal above T_c associated also with pair formation by tunneling measurements [29].

As the temperature decreases below $T_{on}(p)$ some grains become superconductors, the zero resistivity transition takes place when the Josephson coupling E_J among these grains is sufficiently large to overcome thermal fluctuations [30]. Thus $E_J(p, T = T_c) \approx k_B T_c(p)$ what leads to phase locking and long range phase coherence. Consequently the superconducting transition in cuprates occurs in two steps, similar to a superconducting material embedded in a non superconducting matrix [30]: First by the appearing of intragrain superconductivity and by Josephson coupling with phase locking at a lower temperature, *what provides a clear interpretation to the presence of the superconducting amplitude $\Delta_d(i, T)$ above $T_c(p)$.*

The Cuprates Phase Diagram. – In this approach $T_c(p)$ is not directly related with the intragrain superconductivity, and the amplitudes $\Delta_d(i, T)$ do not change appreciably around $T_c(p)$, specially for underdoped compounds, characterized by very large $T_{on}(p)$. This consequence of the present granular theory has been experimentally verified by temperature dependent tunneling [31] and angle resolved photon emission [32]. Using to the theory of granular superconductors [33] to the electronic grains,

$$E_J(p, T) = \frac{\pi\hbar}{4e^2 R_n} \tanh\left(\frac{\Delta(T, p)}{2k_B T_c}\right). \quad (4)$$

Where $\Delta(T, p)$ is the average of the BdG superconducting gaps calculations $\Delta_d(i, T)$ on a 24×24 square taken from the 105×105 mesh after the CH simulations as that shown in Fig.(1). The R_n is the normal resistance of a given compound, which we take as proportional to the ρ_{ab} measurements [34] on the complete series of $La_{2-p}Sr_pCuO_2$. These R_n values are given in the legend of the Fig.(2) top panel. The average $\Delta(T, p)$ as function of p are plotted in the low panel of Fig.(2) with the $T_c(p)$ results from Eq.4) are in the inset and yields the well known dome shape with excellent agreement with the Bi2212 values. This is one of the most important result of our CH-BdG calculations.

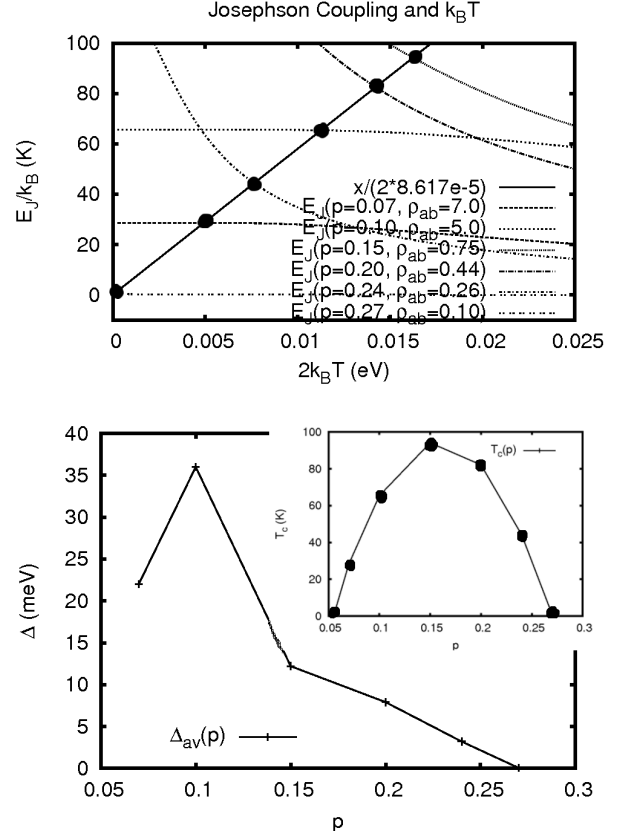


Fig. 2: In the top panel we plot $k_B T$ and the Josephson coupling among superconducting grains $E_J(p, T)$ for some selected doping values as function of T . The curves intersections give the dome shaped $T_c(p)$, as plotted in the inset in the down panel where we show the average $\Delta(T, p)$ calculations.

The STM Results and Interpretation. – According to the recent STM data [9, 10], the low values of $T^*(p) \sim T_{PS}(p)$ for overdoped samples rules out any ionic mobility as the origin of the inhomogeneities in overdoped samples and probably at all dopings. Thus we want to show that these STM results can be interpreted by the granular behavior resulting from the EPS, calculating the symmetric local density of states (LDOS) at different local doping,

$$N_i(E) = \sum_n [|u_n(\mathbf{x}_i)|^2 + |v_n(\mathbf{x}_i)|^2] \times [f'_n(E - E_n) + f'_n(E + E_n)], \quad (5)$$

where f_n is the Fermi function, the prime is the derivative with respect to the argument, and u_n, v_n and E_n are respectively the eigenvectors and positive eigenvalues (quasi-particles exciting energy) of the BdG matrix equation [14, 20, 22, 23, 25].

Here we concentrate on a $p = 0.23$ compound that is close to the Bi2212 compounds used in recently STM ex-

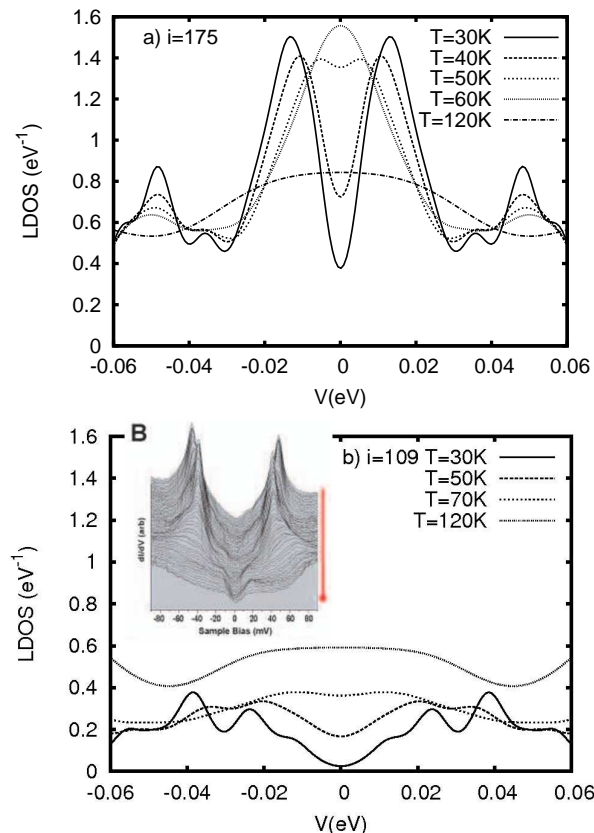


Fig. 3: In the panel a) we plot the LDOS at a "metallic" site ($i=175$) inside a high density grain with $\Delta(T=30K) = 17\text{meV}$. As the temperature increases the coherent gaps close (at $T \approx 52\text{K}$). In panel b) we show a LDOS with an "insulator" grain ($i=109$) which has both $p(i)$ and $\Delta(T=0)$ almost zero. At $T=120\text{K}$ both LDOS converges to the same value all over the plane because the proximity to $T_{PS} = 140\text{K}$. The inset shows the low temperature STM data of McElroy et al [8] displaying the same behavior of our calculations.

periments with many novel results [9, 10]. The low temperature CH EPS calculations on this sample with the estimated value of $T_{PS} = 140\text{K}$ yield that $\approx 20\%$ of the sites are in very low densities regions with $p(i) < 0.05$. These low density unitary cells have quite distinct LDOS behavior than the high density ones as it is shown in Fig.(3).

The calculations at sites in the high density regions have larger superconducting amplitudes $\Delta(i, T)$ with well defined (coherent) and high LDOS peaks. $\Delta(i, T)$ is calculated directly from the BdG equations but can be also estimated by the position of the first LDOS peak. As the temperature increases, it shows the closing of these peaks and the building up of spectral weight at the Fermi level ($E=0$) (Fig.(3a)). In particular, for this case, we have a $\Delta(0, i=175) \approx 17.7\text{meV}$ and the gap derived from the peaks decreases and closes near $T=52\text{K}$. This behavior is quite common to the sites with $p(i) > 0.05$ and with

$T_c(i)$ around 45K and 60K.

On the other hand, the calculations at points with $p(i) < 0.05$ display a rather different behavior as it is shown in panel b). As an example we show the LDOS at $i=109$ with $p(i) \approx 0$ and $\Delta(0, i=109) \approx 0$. It shows a much smaller LDOS (compare the vertical scale of panel a) and b)) without the low temperatures coherent peaks as in panel a) and with small oscillations far from the Fermi energy given an impression of a larger (incoherent) gap. These small oscillations followed by other peaks are quite similar to the firsts few peaks in the work of McElroy et al [8] showing in the inset of panel b). As the temperature increases and reaches $T=50\text{K}$ we see that the LDOS at panel a) is almost close yielding a $\Delta(i=173, t=50K) \sim 0$ while the LDOS at panel b) has still a large dip that gives a $\Delta(i=109, t=50K) \sim 20\text{meV}$. This dip in the LDOS stays much above the resistivity transition $T_c = 60\text{K}$ in close agreement with the STM maps of Gomes et al [9].

Since the V_{GL} potential (Eq.(3)) vanishes with the order parameter, the LDOS for both cases converge to the same value as the temperature approaches the "melting" temperature $T_{PS} = 140\text{K}$, as it is demonstrated in the Fig.(3) by the $T=120\text{K}$ curve.

Another striking result of the CH-BdG calculations is that, despite the uncertainty on $T_c(i)$ (or T_p in the notation of Gomes et al [9]) for very small gaps, mostly of our results follow close the measured relation $2\Delta_d/K_B T_c(i) \approx 7.9$ [9]. For the case of $i=175$, $T_c(i) = 52\text{K} = 4.5\text{meV}$ and $2\Delta_d(i, 0) = 34\text{meV}$ which gives a ratio of 7.6. For $i=109$, taking the first peak in Fig.(3b) at 26meV which closes completely at $T \approx 74\text{K}$, we obtain again $2\Delta/K_B T_c(i) \approx 8.1$ again in close agreement with the STM data [9] but larger than the value measured by tunneling of $2\Delta_d/K_B T_c(i) \approx 6.0$ [29]. Since the lower density (insulator) grains have much smaller LDOS around the Fermi level, they also have lower local conductivity, although the gaps measured by the position of the LDOS peaks, as discussed above, are larger than high density sites with their coherent peaks. Consequently regions with larger gaps have lower conductivity as it was recently measured [10].

Conclusion. – In summary we have made a detailed study of the EPS in HTSC using the CH theory that allows us to followed the local free energy minima that generate the high and low density grains in the Cu-O planes. The differences in these free energy local minima were calculated numerically and used in the BdG approach as the superconducting interaction in the electronic grains of cuprates in the non adiabatic limit. These calculations give rise to the intragrain superconductivity and they provide a scenario to the pseudogap phase, as composed of local regions with finite superconducting amplitude $\Delta(i, p, T)$ without phase locking. The Josephson coupling calculations in connection with the measured values of the resistivity yield an accurate $T_c(p)$ curve for the whole doping values of the Bi2212 series. The LDOS calculated in the high density grains yield the coherent peaks,

and those in the low density regions give larger gaps and ill defined peaks in agreement with the STM data in Bi2212. As far as we know, this present work is the only one to give an interpretation to all the whole STM results.

All of these calculations in close agreement with current data led us to conclude that the EPS is an important ingredient above the superconducting phase and generates mostly of all the intricate normal phase physics of the HTSC.

I gratefully acknowledge partial financial aid from Brazilian agency CNPq.

REFERENCES

- [1] TRANQUADA J.M. ET AL, *Nature (London)*, **375** (1995) 561.
- [2] BIANCONI A. ET AL, *Phys. Rev. Lett.*, **76** (1996) 3412.
- [3] BOZIN E.S. ET AL, *Phys. Rev. Lett.*, **84** (2000) 5856.
- [4] UEMURA Y.J., *Sol. Stat. Comm.* , **126** (2003) 23.
- [5] SONIER J.E. ET AL, *Phys. Rev. Lett.* , **101** (2008) 117001.
- [6] SINGER P.M., HUNT A.W., and IMAI T, *Phys. Rev. Lett.* , **88** (2002) 47602.
- [7] GRAFE H.J. ET AL, *Phys. Rev. Lett.*, **96** (2006) 017002.
- [8] MCELROY K. , ET AL, *Phys. Rev. Lett.*, **94** (2005) 197005.
- [9] GOMES KENJIRO K. ET AL, *Nature* , **447** (2007) 569.
- [10] PASUPATHY ABHAY N. ET AL, *Science* , **320** (196) 2008.
- [11] GORKOV L.P. and SOKOL A.V., *JETP Lett.* , **46** (1987) 420.
- [12] YUKALOV V.I. and YUKALOVA E.P., *Phys. Rev. B*, **70** (2004) 224516.
- [13] EMERY V.J. and KIVELSON S.A., *Physica C*, **209** (1993) 597.
- [14] DE MELLO E.V.L, PASSOS C.A.C and KASAL R.B., *J. Phys.: Condens. Matter*, **21** (2009) 235701.
- [15] TIMUSK T. and STATT B., *Rep. Prog. Phys.* , **62** (1999) 61.
- [16] TALLON J.L. and LORAM J.W, *Physica C*, **349** (2001) 53.
- [17] DE MELLO E.V.L. ET AL, *Phys. Rev. B*, **67** (2003) 024502.
- [18] CAHN J.W. AND HILLIARD J.E. , *J. Chem. Phys*, **28** (1958) 258.
- [19] DE MELLO E.V.L. , AND SILVEIRA FILHO OTTON T. , *Physica A*, **347** (2005) 429.
- [20] DE MELLO E.V.L. and CAIXEIRO E.S., *Phys. Rev. B*, **70** (2004) 224517.
- [21] BRAY A.J. , *Adv. Phys.*, **43** (1994) 347.
- [22] DE MELLO E. V. L. and DIAS D. N., *J. Phys.C.M.* , **19** (2007) 086218.
- [23] DIAS D. N. ET AL, *Physica C*, **468** (2008) 480.
- [24] DE MELLO E.V.L. ET AL, *Proceedings of SCES08, Physica B* (2009) .
- [25] CAIXEIRO E.S, DE MELLO E.V.L., and TROPER A., *Physica C*, **459** (2007) 37.
- [26] DE MELLO E.V.L. and RANNINGER J., *Phys. Rev.B*, **55** (.) 1997 14872
- [27] BEHNIA KAMRAN, *J. Phys.:Condens. Matter*, **21** (2009) 113101.
- [28] WANG YAYU , LI LU and ONG N. P., *Phys. Rev. B* , **73** (2006) 024510.
- [29] MOURACHKINE A., *Mod. Phys. Lett. B*, **19** (2009) 743.
- [30] MERCHANT L. ET AL, *Phys. Rev.B*, **63** (2001) 134508.
- [31] SUZUKI MINORU and WATANBE TAKAO , *Phys. Rev. Lett*, **85** (2000) 4787.
- [32] KANIGEL A. ET AL, *Phys. Rev. Lett.*, **101** (2008) 137002.
- [33] AMBEOGAKAR V. and BARATOFF A., *Phys. Rev. Lett.* , **10** (1963) 486.
- [34] TAKAGI H. ET AL, *Phys. Rev. Lett.* , **69** (1992) 2975.